DOI: 10.1002/ejoc.200600650

Synthesis and Conformational Analysis of Constrained β-Turn Mimetics Incorporating a Bicyclic Turn Inducer by Use of the Petasis Three-Component Reaction on Solid Phase

Elisa Danieli,[a] Andrea Trabocchi,[a] Gloria Menchi,[a] and Antonio Guarna*[a]

Keywords: Peptidomimetics / Scaffold / Amino acids / Solid-phase synthesis

A new set of β-turn mimetics incorporating a bicyclic turn inducer was achieved by use of the solid-phase Petasis reaction in a stereoselective fashion. The stereoselectivity of the reaction turned out to be dependent on the side chain of the amino acid preceding the reverse turn inducer. The β-turn mimetics were stabilized by strong intramolecular 10-membered ring hydrogen bonds, detected by conformational analysis by NMR and molecular modelling, whilst the turn type was controlled by the final amine component. Use of arylboronic acids provided access to chemical diversity at position $i+1$, whilst the versatility of the HMBA resin allowed additional diversification to be introduced at the cleavage stage, thus providing a tool for the generation of libraries of β-turn mimetics as privileged structures in combinatorial chemistry.

Introduction

The generation of reverse turn systems is an important aspect of peptidomimetics research, as these arrangements of amino acids are often sources of biological activity in the contexts of protein–protein and peptide–protein interactions.[1] In particular, β-turns are key elements in molecular recognition mechanisms, because they allow two to four side chains of amino acids involved in biological interactions to be oriented in a stereocontrolled fashion. The development of mimetics of secondary structures such as β-turns and β-sheets has been intensely investigated, and several organic templates that function as turn mimetics have been reported.[2,3] The typologies of reverse turn mimetics can be grouped into two main classes: a) peptidomimetic compounds showing structural analogies with native β-turns and containing similar functional groups,[2] and b) molecular scaffold mimetics of the central dipeptidic $i+1$ to $i+2$ sequence in a turn, capable of inducing folded structures with conformations stabilized by intramolecular hydrogen bonds.[3] In this context there have been several examples of the use of solid-phase methods for the construction of libraries of turn mimetics capable of carrying substituents in place of the side chains at positions $i+1$ and $i+2$,[4] and interesting applications of β-turn mimetics in medicinal chemistry have been reported.[2d,5] Our previous efforts in the development of constrained reverse turn inducers have focused on the synthesis and conformational analysis of bicyclic scaffolds capable of acting either as isosteres of the central $i+1$ to $i+2$ dipeptide sequence in a β-turn,[6] or as constrained bicyclic proline mimetics introduced at positions $i+1$ (type I/II β-turn mimetics) or $i+2$ (type VI β-turn mimetics).[7] Recently, enlarged bicyclic templates have been reported by our group to function as unusual reverse turn inducers, and it was demonstrated that a stable hydrogen-bonding network contributed to create a β-sheet-like structure.[8] Following the concept of chemical diversity, we set out to expand the scope of these dipeptide isosteres as turn inducers, as reported previously,[6c] through the use of the Petasis reaction to introduce an additional carbon atom as a point of diversity at position $i+1$, thus allowing the generation of collections of new β-turn mimetic systems. The Petasis, or Mannich-boronic, reaction is a three-component reaction between an amine, a boronic acid and glyoxylic acid, which permits the generation of α-amino acid compounds (Scheme 1).[9]

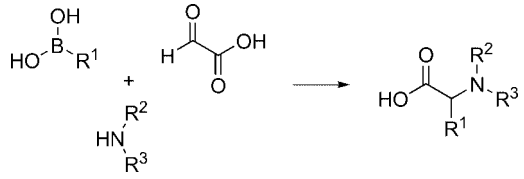

Scheme 1. Petasis reaction for the synthesis of α-amino acids.

Some examples from the literature include methods for the solid-phase application of the Petasis reaction in peptidomimetic chemistry;[10] in particular, Golebiowsky et al.

[a] Dipartimento di Chimica Organica "Ugo Schiff", and Laboratorio di Progettazione, Sintesi e Studio di Eterocicli Biologicamente Attivi (HeteroBioLab), Università degli Studi di Firenze,
Via della Lastruccia 13, 50019 Sesto Fiorentino, Italy
Fax: +39-055-4573569
E-mail: antonio.guarna@unifi.it

have also reported on the synthesis of β-turn mimetics[11] allowing for diversification around position $i+1$. In this paper we report a method for the generation of 10-membered ring hydrogen-bonded structures (Figure 1, right) through application of the Petasis reaction.

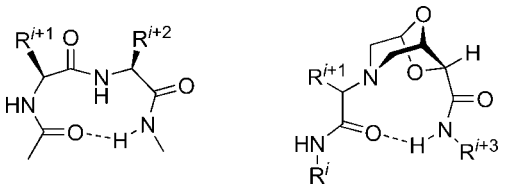

Figure 1. β-Turn (left) and β-turn mimetic (right) structures.

Such a structure, although representing a complete modification of the $i+1$ to $i+2$ dipeptidic sequence, was capable of mimicking the ten-membered ring hydrogen-bonded structure typical of β-turns. Moreover, elements of diversity could be introduced at position $i+1$ through the use of the three-component reaction, and at positions i and $i+3$ through the use of different amines as building blocks. Conformational analysis of selected compounds to investigate the structural features of the new β-turn mimetics was successively carried out by NMR and molecular modelling techniques.[12] In particular, TOCSY and ROESY spectra were recorded to assign proton resonances and to investigate both sequential and long-range NOEs that might provide evidence of preferred conformations and give insight into stable reverse turn conformations.[13] Temperature-dependence experiments were also carried out, since amide proton chemical shifts are sensitive to temperature and dilution variations,[14] and the combination of chemical shifts and $\Delta\delta/\Delta T$ coefficients of the amide protons can provide information on the extent of hydrogen bonding. Moreover, the $\Delta\delta$(NH) variation upon addition of a solvent such as DMSO, capable of competing in the formation of hydrogen bonds, was also evaluated to test further the role of amide protons in forming stable intramolecular hydrogen bonds. Molecular modelling calculations were used to assess the conformational preferences of the reverse turn structures. In particular, Monte Carlo conformational searches[15] were performed to scan all the conformational space accessible to the molecules, whilst molecular dynamics calculations were carried out to investigate the strengths of hydrogen-bonded structures and to verify the stabilities of the preferred conformations around the local minima.

Results and Discussion

The synthesis of the molecules of general structure as shown in Figure 1 (right) was carried out either on Wang resin or on the base-labile HMBA resin, the latter allowing the introduction of an additional site of chemical diversity at position $i+3$ through the choice of different amines for the nucleophilic cleavage. For the reverse turn inducer, the bicyclic scaffold shown in Scheme 2, prepared by our group as reported previously,[16] was chosen, as the *endo* configuration of such a γ/δ-amino acid allowed the generation of a 10-membered ring hydrogen bond typical of a β-turn. The resin-bound bicyclic turn inducer **1** was thus amine-deprotected and subjected to a solid-phase Petasis reaction to introduce the $i+1$ amino acid mimetic moiety.

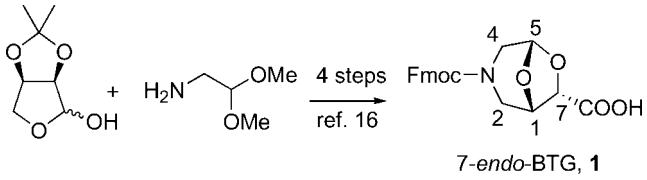

Scheme 2. Scaffold selected as reverse turn inducer.

The synthesis of **2** is representative: coupling of **1** on the resin-bound amino acid was achieved with the aid of HBTU/HOBt as the activating mixture and DMAP as the catalytic base, whilst the outcome of the reaction was monitored by the bromophenol blue (BB) colorimetric test for amines (Scheme 3).[17]

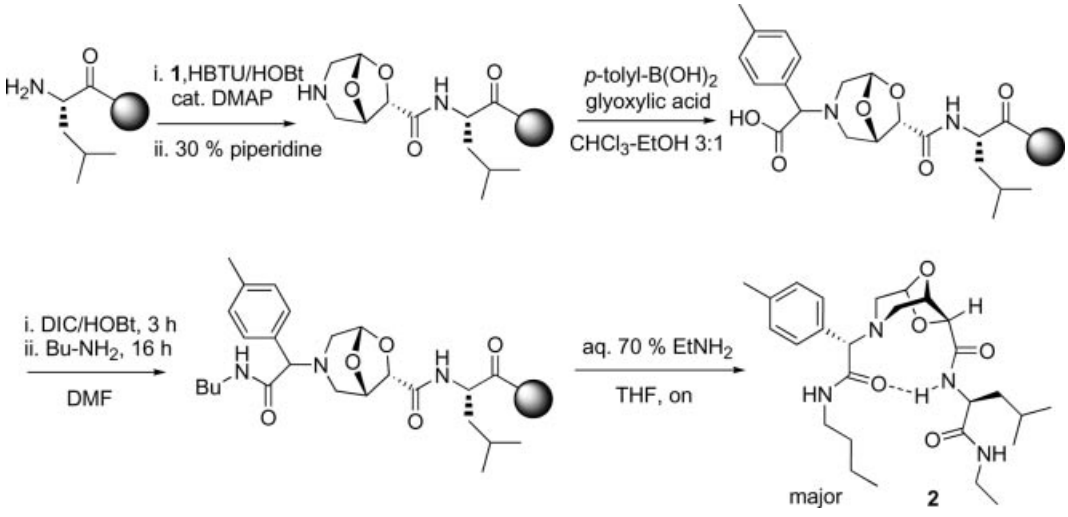

Scheme 3.

After Fmoc removal, the amine function in the bicyclic scaffold was treated with 10 equiv. each of arylboronic acid and glyoxylic acid in a 3:1 mixture of chloroform/ethanol as solvent system. The reaction proceeded at 50 °C, and the presence of the carboxylic group was detected by the specific malachite green (MG) test, as reported by Taddei et al.[18] Finally, amide bond formation was obtained by carboxylic group activation with DIC/HOBt, followed by addition of the amine component.[19] The final β-turn mimetic was obtained after cleavage from the resin by use of an excess of amine, giving **2** in 30% overall yield as a mixture of diastereomers in 84% *de*. Table 1 reports selected examples of turn molecules of general formula as in Figure 2. Use of Wang resin and 7-*endo*-BTG allowed a structure with the COOH group at the C-terminal position to be obtained (Entry 4), whereas by use of HMBA resin it was possible to obtain the same compound as a C-terminal ethylamide, by nucleophilic cleavage with 70% aqueous $EtNH_2$ in THF. In order to develop a general procedure to provide additional diversity within C-terminal amides, a different workup was developed when other amines were used. Specifically (see Entry 6), the excess of unreacted amine was treated for 30 minutes with cheap, commercially available L-di-*O*-acetyltartaric anhydride as scavenger, and the mixture was then eluted through a column of basic Ambersep-OH resin to remove the resulting amido acid.

Table 1. Yields and *de* ratios of selected β-turn mimetics.

Entry	R^1	X	R^2	R^3		*de* [%][a]	Overall yield [%][b]
1	–NHEt	–	*p*-tolyl	–NHBu	**3**	5	15
2	–NHEt	Leu	*p*-tolyl	–NHBu	**2**	84	30
3	–NHEt	Leu	*p*-tolyl	–Phe-NHEt	**4**	89	13
4	–OH	Leu	*p*-tolyl	–NHBu	**5**	61	11
5	–NHEt	Gly	*p*-tolyl	–NHBu	**6**	49	22
6	–NHBn	Val	*p*-tolyl	–NHBu	**7**	30	7
7	–NHEt	Phe	*p*-Cl-Ph	–NHBu	**8**	20	16

[a] Determined by HPLC analysis. [b] Based on resin loading as reported by the manufacturer.

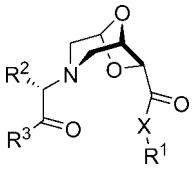

Figure 2. General structure of β-turn mimetics **2**–**8**.

The bicyclic turn inducer was also mounted directly on the resin to provide the minimal β-turn mimetic **3** with a *de* of only 5%, as a result of absence of diastereoselectivity in the Petasis reaction (Table 1, Entry 1). Interestingly, compounds **2** and **4**–**8** (Entries 2–7) represented varying degrees of diastereoselection, in line with some other examples of the diastereoselectivity and enantioselectivity of the Petasis reaction reported in the literature.[9a,20] In particular, compounds **2** and **4** (Entries 2 and 3, respectively), with leucine at position 7 in the bicyclic turn inducer, showed *de*s of 84% and 89%, respectively, thus mainly consisting of the compounds possessing (*S*) configurations at their newly generated stereocenters, as evidenced by ROESY data (see below).[21] In contrast, turn mimetics with different amino acids preceding the bicyclic turn inducer showed lower *de* values (Entries 5–7), indicating a role of the side chain of the preceding amino acid in the stereoselectivity outcome, although this effect could not be exclusive, as a glycine-containing turn mimetic (Entry 5) showed a higher *de* value than a valine-containing turn mimetic **7** (Entry 6). Thus, as well as the stereochemical information at C_α in the preceding amino acid X (Figure 2), the existence of an additional effect was also implied as a possible explanation of the mechanism resulting in the diastereoselective Petasis reaction. It was hypothesized that, given the preference for *exo* attack of the aryl moiety on the iminium function with respect to the bicyclic skeleton due to steric hindrance, the diastereoselectivity might be governed by the isomerism of the intermediate iminium double bond at N-3. According to earlier works,[6a] the geometry of the C=O group at C-7 is essentially *anti* with respect to the C-7–O-6 bond, so the constraint generated by the amide bond at C-7, in conjunction with the rigid structure of the bicyclic scaffold, might generate a stabilized asymmetric conformation capable of differentiating the two faces of the iminium species towards the nucleophilic attack by the anionic species of the boronic component (Figure 3). Specifically, the intermediate structure (Figure 3, bottom left) should experience greater steric hindrance than the structure (Figure 3, top left) giving rise to the major compound possessing the (*S*) configuration at the newly generated stereocenter (Figure 3, top right). Finally, the *de* outcome turned out to be dependent on the conformational preferences of the overall peptidomimetic system, which could in turn be governed by the side chain

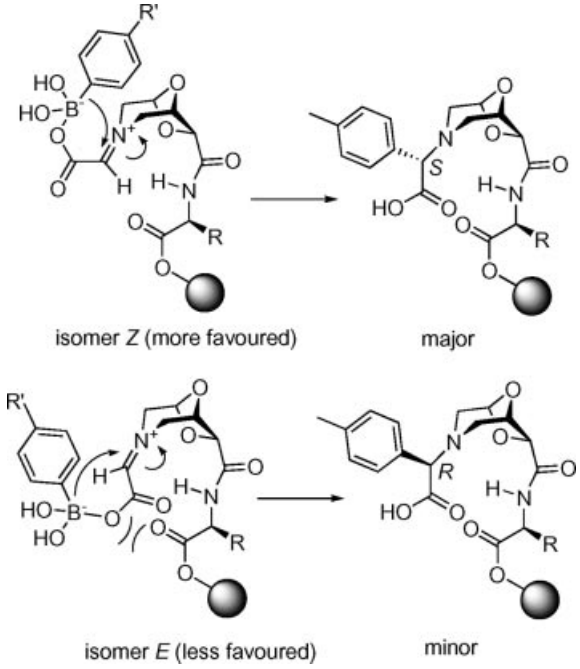

Figure 3. Putative mechanism for the diastereoselective outcome of the Petasis reaction.

of the amino acid at position X (see Figure 2 and Table 1, Entries 2–7). Such a rigid conformation would not have been able to exist when the bicyclic amino acid was linked to the resin as an ester (Table 1, Entry 1), consistently with the lack of diastereoselectivity observed for **3**, resulting in an undifferentiated *exo* attack of the aryl moiety at both faces of the iminium species.

Conformational Analysis

In order to establish the reverse turn properties of the new molecules, a conformational analysis of selected compounds by NMR and molecular modelling was carried out. In particular, the conformational preferences of the major diastereomers of compounds **2** and **4** were assessed in 4 mM and 3.3 mM $CDCl_3$ solutions, respectively (Figure 4).[22] Furthermore, molecular modelling was carried out to corroborate the NMR spectroscopic data and, specifically, Monte Carlo conformational searches[15] were performed to scan all the accessible structures within an energy range of 24 kJ mol^{-1}, whilst the minimum energy structures were subjected to a mixed dynamics simulation by the Monte Carlo/Stochastic Dynamics (MC/SD) approach[23] in order to investigate the conformations available in the vicinity of local minima. Variable-temperature ^{1}H NMR spectroscopy on compound **2** revealed the presence of a strongly hydrogen-bonded structure. In fact, although all the $\Delta\delta/\Delta T$ values for the three amide protons of **2** proved to be small in absolute value, the leucine amide proton (10-H) showed a significant deshielded chemical shift, indicative of the presence of a strong hydrogen bond, whereas low chemical shifts for the other amide protons (8-H and 12-H) suggested the absence of any hydrogen-bonded conformation within the range of temperatures examined (Table 2).

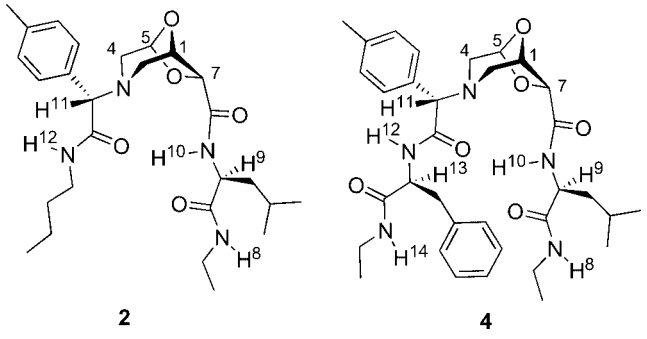

Figure 4. Turn mimetics selected for conformational analysis.

Such a hypothesis was confirmed by ^{1}H NMR experiments with **2** in $CDCl_3$ solutions recorded with increasing amounts of [D_6]DMSO as a hydrogen bond competitor (Figure 5). In fact, only 10-H showed any significant stability of its chemical shift in the presence of increasing amounts of [D_6]DMSO, whereas the other two amide protons each displayed a downfield shift of more than 0.2 ppm in a 10% mixture of [D_6]DMSO in $CDCl_3$. These data suggested that the ethyl (8-H) and butyl (12-H) amide protons were solvent-exposed and interacted with the competing solvent in the generation of intermolecular hydrogen bonds, thus resulting in deshielding of their chemical shifts.

Table 2. Temperature-dependent ^{1}H NMR spectroscopic data for amide protons in compounds **2** and **4** (see Figure 4).

	Amide proton	δ[b]	$\Delta\delta/\Delta T$[c]
2[a]	12-H	6.23	–1.78
	10-H	7.61	–0.78
	8-H	6.30	–0.71
4[a]	14-H	6.32	–5.00
	12-H	7.92	–6.64
	10-H	6.87	–1.64
	8-H	7.71	–9.64

[a] Spectra were recorded in $CDCl_3$ within the ranges of 23–53 °C for **2** and 20–50 °C for **4**. [b] Chemical shifts (δ) are expressed in ppm. [c] Temperature coefficients ($\Delta\delta/\Delta T$) are expressed in ppb K^{-1}.

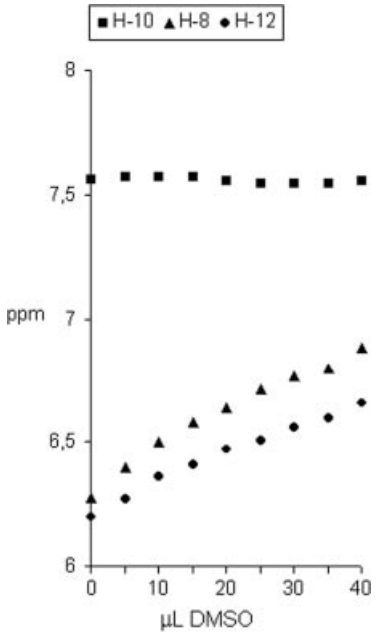

Figure 5. Diagram of ^{1}H NMR chemical shifts upon [D_6]DMSO addition to a $CDCl_3$ solution (4 mM) of **2**.

Amide proton–deuterium exchange rates were assessed to provide further supporting evidence for the role of the leucine amide 10-H in generating a stable intramolecular hydrogen-bond.[24] Exchange rates with deuterated methanol, with a 3:1 $CD_3OD/CDCl_3$ solution of **2**, demonstrated the exceptional stability of the leucine NH hydrogen bond, as its NMR signal was still present after 2 h, whereas the other two protons exchanged with deuterium instantly. ROESY experiments provided additional information relating to the conformational preferences of compound **2**. The major stereoisomer was found to possess the (*S*) configuration at the C-11 stereocenter bearing the *p*-tolyl group, as corroborated by the ROESY peaks of the 11-H and 2-H protons of the scaffold (Figure 6) and by ROESY correlations of 4-H and the aromatic protons of the tolyl group.

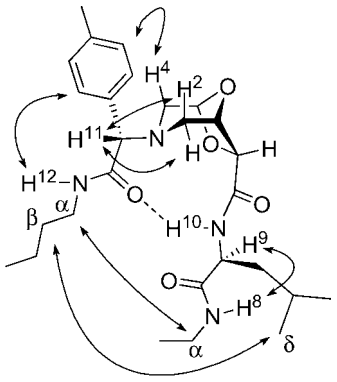

2

Figure 6. ROESY correlations for compound **2**.

A strong cross-strand peak between Leu δ-H and butyl β-H, together with medium ROESY peaks between the α-H protons of the butyl and ethyl groups, demonstrated the turn geometry of compound **2**. In addition, the medium ROESY correlation between 12-H and the aromatic protons of the *p*-tolyl group confirmed the proposed hydrogen-bonded structure for **2**, as shown in Figure 6, with the butyl amide proton pointing outside the turn, consistently with variable-temperature experiments. Molecular modelling calculations were performed to corroborate the NMR spectroscopic data and to provide further insights into the conformational preferences of turn mimetic **2**, with the use of full unconstrained Monte Carlo conformational analysis with $MM2^+$ as a force field, together with the implicit chloroform GB/SA solvation system.[25] The calculations showed the existence of two main conformations, each possessing a β-turn mimetic structure and stabilized by a ten-membered ring hydrogen bond. The first minimum-energy conformer was inconsistent with the NMR spectroscopic data, as the hydrogen bond between the butyl NH and the carbonyl group at the C-7 position in the bicyclic scaffold was not supported either by ROESY data or by the ^{1}H NMR spectra after [D_6]DMSO addition. The second conformer (Figure 7) was found in 17.2% of the generated structures and showed a turn structure stabilized by a ten-membered ring hydrogen bond between Leu NH (10-H) and the glyoxylic acid carbonyl group, fully consistently with NMR spectroscopic data (Figure 6). MC/SD simulation on compound **2** was performed over 1000 ps, yielding 1000 samples for each ps of the calculation. Under these conditions, only the second conformer (as shown in Figure 6) was found, in 11.5% amount among the generated structures, indicating a better agreement with all the ROESY correlations.

Conformational analysis of compound **4** showed a different structural preference, indicating a possible role of phenylalanine in the selection of the most accessible conformations. Variable-temperature experiments showed the existence of equilibrating conformations. In fact, chemical shift values and high $\Delta\delta/\Delta T$ coefficients for 12-H and 8-H amide protons indicated the presence of equilibrating hydrogen-bonded and non-hydrogen-bonded conformations (see Figure 4, right and Table 2). Although showing a low temperature coefficient with respect to the other amide protons in the molecule, leucine 10-H also displayed a lower chemical shift relative to the same amide proton as in compound **2**, and a non-hydrogen-bonded state for that proton was assumed. ^{1}H NMR spectroscopy on dilute $CDCl_3$ solutions of **4** in the presence of increasing amounts of [D_6]DMSO as a hydrogen bond competitor showed small chemical shift deviations for the amide Phe 12-H and 8-H protons, suggesting their role in the generation of stable intramolecular hydrogen bonds (Figure 8).

Figure 7. Low-energy conformation for β-turn mimetic **2**.

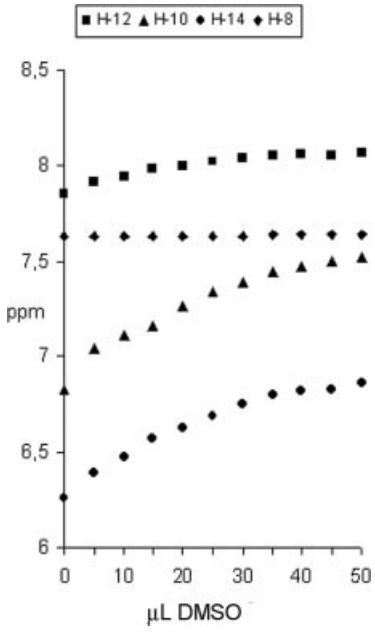

Figure 8. Diagram showing ^{1}H NMR chemical shifts upon [D_6]-DMSO addition to a 3.5 mM $CDCl_3$ solution of **4**.

Specifically, the existence of an intramolecular hydrogen bond between 12-H and the carbonyl group at C-7 of the bicyclic compound was suggested, giving a shifted β-turn structure with respect to the hydrogen-bonded structure of **2**. Such a hydrogen-bonded structure resembled the β-turn structure as in Figure 1 (left), with the bicyclic turn inducer **1** at position $i+1$ and the *p*-tolyl group at position $i+2$ in a reversed fashion with respect to the structure observed for **2** (Figure 9 for **4**; cf. Figure 6 for **2**).

A ROESY experiment with compound **4** showed the major stereoisomer to possess the (*S*) configuration at the

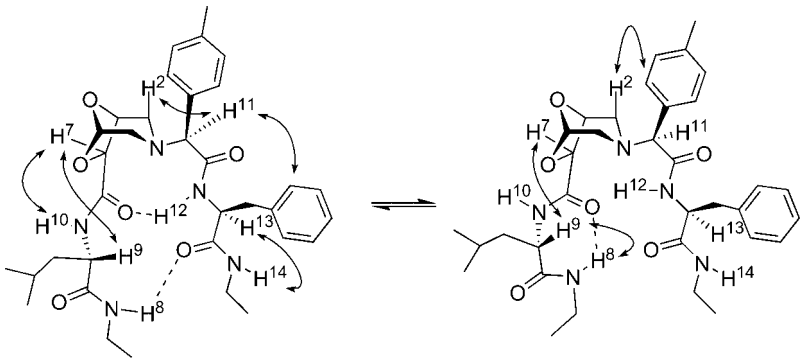

4

Figure 9. ROESY correlations for reversed conformation of β-turn mimetic **4**.

C-11 stereocenter bearing the tolyl group ($i+2$ position as referred to Figure 9), in analogy with **2**, as demonstrated by the ROESY peaks of the 11-H and 2-H protons of the scaffold (Figure 9, left). An intense ROE contact between 10-H and 7-H indicated that the scaffold carbonyl group was pointing inside the turn, thus demonstrating the existence of the hydrogen bond originating from 12-H, as shown in Figure 9 (left). Moreover, ROESY peaks between the aromatic protons of the *p*-tolyl ring and 2-H, and also between 9-H and 7-H (Figure 9, right), indicated a certain rotational freedom of the two halves of the turn structure, thus corroborating the large $\Delta\delta/\Delta T$ coefficients obtained from variable-temperature NMR experiments and confirming the existence of equilibrating hydrogen-bonded and non-hydrogen-bonded conformers about the 12-H and 8-H amide protons. Such conformational freedom was also demonstrated by the absence of significant cross-strand ROESY peaks, probably as a result of steric hindrance by the phenylalanine moiety. ROESY peak between 9-H and 7-H also suggested the existence of a γ-turn structure stabilized by a hydrogen bond between 8-H and the carbonyl group at C-7 of the bicyclic scaffold, as shown in Figure 9 (right).

Molecular modelling calculations confirmed the different structural organization for **4**. In particular, Monte Carlo conformational analysis showed the existence of the hydrogen-bonded conformation as shown in Figure 9 (left), corresponding to the global minimum, consistently with the NMR spectroscopic data. Such a conformation was present in 82% of the structures found within the range up to 6 kcal mol^{-1} above the global minimum energy. The MC/SD calculation confirmed the preference for the hydrogen-bonded structure corresponding to the global minimum, as also shown in Figure 10, though the amount of the minimized structures dropped to 15.4%, in better agreement with NMR spectroscopic data indicating the existence of equilibrating conformations for **4**. Moreover, the proposed γ-turn structure as in Figure 9 (right) was satisfied by 60.4% of the structures, confirming the substantial preference of 8-H amide proton for hydrogen-bonded states, as corroborated by ROESY data and ^{1}H NMR spectra upon addition of [D$_6$]DMSO.

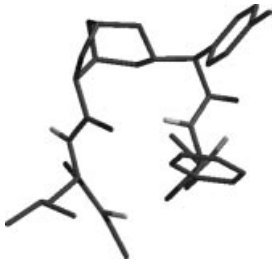

Figure 10. Global minimum conformation for β-turn mimetic **4** shown in reversed conformation as in Figure 9.

Conclusions

This work reports a solid-phase methodology for the generation of a collection of β-turn mimetics based on employment of a bicyclic reverse turn inducer and use of the Petasis reaction to introduce diversity at position $i+1$. This synthetic strategy allowed the generation of small molecules with conformational profiles typical of β-turns, with the potential to vary five positions in the turn mimetic. Moreover, the Petasis reaction showed a degree of diastereoselectivity depending on the amino acid preceding the reverse turn scaffold, thus suggesting a role of the bicyclic γ/δ-amino acid in determining the selection of the two possible sides for nucleophilic attack in the three-component process. Specifically, it is hypothesized that the amide bond between the bicyclic scaffold and the preceding amino acid could provide an asymmetric setting in the overall molecular structure, and that this could in turn govern the stereoselectivity observed in the Petasis reaction. Finally, conformational analysis of two selected structures revealed that the type of β-turn mimetic stabilized by a ten-membered ring hydrogen bond turned out to be dependent on the amine component coupled to the glyoxylic COOH, as the introduction of phenylalanine in that position shifted the β-turn conformation from a structure stabilized by a ten-membered hydrogen-bond between the glyoxylic C=O and the 10-H amide proton to another one stabilized by a ten-membered hydrogen bond formed by the C=O group at C-7 and the 12-H amide proton. This information may be of interest

for the design of new β-turn mimetics, as the right choice of amine compound for coupling to glyoxylic COOH may make the peptidomimetic system assume a different β-turn conformation.

Experimental Section

General Remarks: HMBA-AM resin (0.83 mmol g^{-1}) was purchased from Novabiochem. Chromatographic separations were performed on silica gel by flash column techniques. R_f values refer to TLC carried out on 25 mm silica gel plates with the same eluent as indicated for column chromatography. All the solid-phase reactions were carried out with use of a shaker, in solvent of HPLC quality. ^1H and ^{13}C NMR spectra were recorded with NMR instruments operating at 200 MHz and 400 MHz for proton and 50.33 and 100.66 for carbon, respectively, in $CDCl_3$ solutions unless otherwise stated. Complete NMR analyses of **2** and **4** were performed with the aid of gCOSY, TOCSY, HSQC and ROESY experiments. One-dimensional ^1H NMR spectra for determining temperature coefficients were acquired with increments of 5 K. Sample temperatures were controlled with the variable-temperature unit of the instrument. EI mass spectra were carried out at 70 eV ionizing voltage. All the β-turn mimetics were characterized by ^1H and ^{13}C NMR, EI-MS or ESI-MS, and HPLC with an analytical C-18 10 μm, 250 × 4.6 mm reverses-phase column, through the use of H_2O/CH_3CN buffered with TFA (0.1%) as eluent, and 10% CH_3CN/5 min then 10–90% CH_3CN/20 min as gradient. Bromophenol blue (BB) tests were performed by the following procedure:[17] a few resin beads were put in a vial and suspended in DMF (0.5 mL), and a solution of bromophenol blue in dimethylacetamide (1%, two drops) was then added. The presence of free amino groups was revealed by the deep blue colour of the resin beads. Malachite green (MG) tests were performed by the reported procedure.[18]

General Procedure with HMBA Resin: HMBA-AM resin (200 mg, 0.17 mmol) was used as starting material. Fmoc removal with a DMF solution of piperidine (30%) over 10 min was performed twice, followed by resin washings with DMF and DCM. Successful deprotection and subsequent coupling reactions were assessed by performing the BB test (positive and negative results, respectively). The coupling of the first amino acid was performed by treating the resin for 12 h in a solution containing the amino acid (0.85 mmol, 5 equiv.), HOBt (115 mg, 0.85 mmol, 5 equiv.), DIC (133 μL, 0.85 mmol, 5 equiv.) and DMAP (2 mg) in DMF (3 mL). The solution was then drained and the resin was washed successively with DMF and DCM. After Fmoc removal, the coupling of the scaffold was performed in the following way: a solution of Fmoc-7-*endo*-BTG-OH (**1**, 191 mg, 0.51 mmol, 3 equiv.), HOBt (115 mg, 0.85 mmol, 5 equiv.), HBTU (314 mg, 0.85 mmol, 5 equiv.) and DIPEA (284 μL, 1.7 mmol, 10 equiv.) in DMF (3 mL) was added to the resin, and the mixture was shaken at room temperature for 3 h. The solution was drained and the resin was washed successively with DMF and DCM. The Petasis reaction was performed with a solution of glyoxylic acid (231 mg, 1.7 mmol, 10 equiv.) and boronic acid (1.7 mmol, 10 equiv.) in $CHCl_3$/EtOH 3:1 (3 mL). The solution was added to the resin and the mixture was stirred at 50 °C for 12 h. Afterwards, the solution was drained and the resin was washed with DCM. The completion of the reaction was assessed by the MG test. Successively, the resin was suspended in a solution of HOBt (115 mg, 0.85 mmol, 5 equiv.) and DIC (133 μL, 0.85 mmol, 5 equiv.) in DMF (3 mL), and the mixture was shaken at room temperature for 3 h, followed by draining of the solution and washing of the resin with DCM. A solution of $BuNH_2$ (84 μL, 0.85 mmol, 5 equiv.) in DMF (3 mL) was then added to the resin and the mixture was shaken at room temperature for 12 h. Finally, cleavage was performed with an aqueous solution (70%) of $EtNH_2$ (1.5 mL) and THF (1.5 mL), and the mixture was stirred at room temperature for 12 h. The solution was then drained and concentrated in vacuo to give a crude compound that was purified by flash column chromatography.

(Butylcarbamoyl-*p*-tolylmethyl)-7-*endo*-BTG-Leu-NHEt (2): Compound **2** was prepared by use of Fmoc-Leu-OH as the first amino acid, and with *p*-tolylboronic acid for the Petasis reaction. The crude peptide was purified by flash column chromatography [EtOAc/petroleum ether (2:1), 0.1% Et_3N, R_f = 0.3] to give pure **2** (26 mg, 30%) as a mixture of two diastereomers in 84% *de*. See Table 3 for NMR spectroscopic data. ESI-MS: *m*/*z* (%) = 541.36 $[M + K]^+$ (12), 525.45 $[M + Na]^+$ (100), 503.45 $[M + 1]^+$ (43). HPLC: t_R = 19.8 and 20.3 min (89% pure). Elemental analysis (%) calcd. for $C_{27}H_{42}N_4O_5$ (502.65): C 64.52, H 8.42, N 11.15; found: C 64.66, H 8.31, N 11.20.

(Butylcarbamoyl-*p*-tolylmethyl)-7-*endo*-BTG-NHEt (3): Compound **3** was prepared by anchoring of the Fmoc-7-*endo*-BTG-OH (**1**) directly to the resin, while *p*-tolylboronic acid was used for the Petasis reaction. The crude peptide was purified by flash column chromatography [EtOAc/petroleum ether (2:1), 0.1% Et_3N, R_f = 0.2] to give **3** (10 mg, 15%) as a mixture of two diastereomers in 5% *de* ^1H NMR ($CDCl_3$, 200 MHz) diastereomers A and B: δ = 7.11 (m, 4 H), 7.04 (br s, 1 H, A), 6.83 (br s, 1 H, B), 6.53 (br s, 1 H, B), 6.37 (br s, 1 H, A), 5.51 (s, 1 H, B), 5.38 (s, 1 H, A), 4.70 (s, 1 H, A), 4.69 (s, 1 H, B), 4.60 (s, 1 H, A), 4.57 (s, 1 H, B), 4.46 (m, 2 H, A and B), 3.75 (s, 1 H, B), 3.70 (s, 1 H, A), 3.50–3.19 (m, 8 H), 3.16 (m, 1 H, A), 3.03 (d, $^2J_{H,H}$ = 11.7 Hz, 1 H, B), 2.84 (d, $^2J_{H,H}$ = 11.7 Hz, 1 H, A), 2.66 (d, $^2J_{H,H}$ = 11.3 Hz, 1 H, B), 2.58 (d, $^2J_{H,H}$ = 12.4 Hz, 1 H, A), 2.47 (d, $^2J_{H,H}$ = 11.7 Hz, 1 H, B), 2.32 (s, 3 H, A), 2.30 (s, 3 H, B), 2.27 (m, 1 H, A), 2.05 (d, $^2J_{H,H}$ = 11.7 Hz, 1 H, B), 1.57–1.38 (m, 4 H), 1.35–1.15 (m, 10 H), 0.93–0.84 (m, 6 H) ppm. ^{13}C NMR ($CDCl_3$, 50.33 MHz): δ = 170.1 (s), 170.0 (s), 169.5 (s), 168.9 (s), 129.2 (s), 129.1 (s), 128.4 (s), 127.8 (s), 120.7 (d, 4 C), 119.8 (d, 2 C), 119.2 (d, 2 C), 100.1 (d), 99.5 (d), 77.1 (d), 76.7 (d), 72.3 (d), 70.4 (d), 53.9 (t, 2 C), 53.1 (d) 51.8 (d), 39.0 (t, 2 C), 34.2 (t), 34.1 (t), 31.2 (t), 30.6 (t), 22.7 (t), 22.0 (t), 20.8 (q), 19.9 (q), 14.5 (t), 13.4 (t), 12.3 (q), 11.3 (q), 5.8 (q), 4.8 (q) ppm. MS: *m*/*z* (%): 389 $[M]^+$ (1.4), 289 (100), 246 (1.7), 218 (4). HPLC: t_R = 17.7 and 17.8 min (88% pure). Elemental analysis (%) calcd. for $C_{21}H_{31}N_3O_4$ (389.49): C 64.76, H 8.02, N 10.79; found: C 64.80, H 8.11, N 10.68.

(1*S*)-[(Ethylcarbamoyl-2-phenylethylcarbamoyl)-*p*-tolylmethyl]-7-*endo*-BTG-Leu-NHEt (4): Compound **4** was prepared as described for **2**. The carboxylic acid obtained from the Petasis reaction was treated with DIC/HOBt, and then with a DMF solution of Phe-OMe·HCl (171 mg, 0.85 mmol, 5 equiv.) and DIPEA (284 μL, 1.7 mmol, 10 equiv.). The crude peptide was purified by flash column chromatography [EtOAc/petroleum ether (2:1), 0.1% Et_3N, R_f = 0.3] to give **4** (14 mg, 13%) as a mixture of two diastereomers in 89% *de*. See Table 3 for NMR spectroscopic data. MS: *m*/*z* (%): 622 $[M]^+$ (1.4), 402 (100), 329 (10), 289 (78). HPLC: t_R = 19.2 and 19.5 min (98% pure). Elemental analysis (%) calcd. for $C_{34}H_{47}N_5O_6$ (621.77): C 65.68, H 7.62, N 11.26; found: C 65.66, H 7.71, N 11.20.

(Butylcarbamoyl-*p*-tolylmethyl)-7-*endo*-BTG-Leu-OH (5): Compound **5** was prepared as reported in the general procedure, but with Wang resin (200 mg, 0.136 mmol) as the solid support. Fmoc-7-*endo*-BTG-OH (**1**) was used as the reverse-turn inducer, Fmoc-

Table 3. Proton and carbon chemical shifts of major diastereoisomers of **2** and **4** in $CDCl_3$ (δ values are in ppm, and the J values in Hz are reported in parentheses).

2[a,b]	^{1}H NMR	^{13}C NMR	**4**[c,d]	^{1}H NMR	^{13}C NMR
1-H	4.58	77.6	1-H	4.51	74.5
2-H	3.16, 2.57	51.8	2-H	2.86 (d, 11.2), 2.51 (d, 11.2)	52.0
4-H	2.71, 2.06	53.3	4-H	2.44 (d, 11.7), 1.91 (d, 11.7)	52.8
5-H	5.36	100.6	5-H	5.30	100.5
7-H	4.41	74.4	7-H	4.39	77.3
11-H	3.76	74.7	11-H	3.71	74.9
p-tolyl arom. H	7.07	129.5, 129.4, 128.7	*p*-tolyl arom. H	6.96 (d, 7.3), 6.84 (d, 7.3)	129.2, 128.9
p-tolyl CH_3	2.30	21.1	*p*-tolyl CH_3	2.23	21.1
12-H	6.23	–	14-H	6.32	–
α-butyl	3.19	39.5	α-Et[e]	3.15–3.11	34.4
β-butyl	1.47	31.6	β-Et[e]	0.91, 0.87	14.5
γ-butyl	1.23	20.1	12-H	7.92 (d, 7.3)	–
δ-butyl	0.87	13.9	13-H	4.40	55.9
10-H	7.61	–	β-Phe	3.21, 3.10	36.6
9-H	4.38	77.7	Phe arom. H	7.23–7.19	129.5, 128.5, 126.7
β-Leu	1.90, 1.53	41.2	10-H	6.87 (d, 6.8)	–
γ-Leu	1.90	30.9	9-H	4.68	52.6
δ-Leu	0.98	22.9, 22.7	β-Leu	1.75–1.59	41.7
8-H	6.30	–	γ-Leu	1.59	25.0
α-Et	3.28	34.6	δ-Leu	1.00 (d, 5.8), 0.97 (d, 5.8)	23.1, 22.5
β-Et	1.12	14.8	8-H	7.71	–
			α-Et[f]	3.32, 3.14	34.4
			β-Et[f]	1.11 (t, 7.32)	14.7

[a] ^{1}H and ^{13}C spectra were recorded at 26 °C in $CDCl_3$ solution (4 mM). [b] Numbering refers to Figure 4 (left). [c] ^{1}H spectra were recorded at 20 °C, and ^{13}C spectra were recorded at 25 °C in $CDCl_3$ solution (3.3 mM). [d] Numbering refers to Figure 4 (right). [e] Ethyl group refers to 14-H. [f] Ethyl group refers to 8-H.

Leu-OH as the first amino acid and *p*-tolylboronic acid for the Petasis reaction. The crude peptide was purified by semipreparative HPLC on a C-18 10 μm, 250 × 4.6 mm reversed-phase column, with H_2O/CH_3CN buffered with TFA (0.1%) as eluent, and 0–90% CH_3CN/40 min as gradient (t_R = 27.0 min) to give **5** (9 mg, 11%) as a mixture of two diastereomers in 61% *de*. ^{1}H NMR ($CDCl_3$, 200 MHz) major diastereomer: δ = 8.90 (br., 1 H), 7.64 (br., 1 H), 7.40–7.13 (m, 4 H), 6.95 (br., 1 H), 5.58 (s, 1 H), 5.18 (m, 1 H), 4.92 (m, 1 H), 4.61 (m, 1 H), 3.76 (s, 1 H), 3.38–3.15 (m, 4 H), 2.85 (m, 1 H), 2.30 (s, 3 H), 2.28 (m, 1 H), 1.75 (m, 3 H), 1.41–1.18 (m, 4 H), 0.92–0.81 (m, 9 H) ppm. ^{13}C NMR ($CDCl_3$, 50.33 MHz) major diastereomer: δ = 171.8 (s), 168.9 (s), 167.4 (s), 131.2 (s), 127.4 (s), 120.7 (d, 2 C), 119.2 (d, 2 C), 99.8 (d), 76.8 (d), 72.9 (d), 68.4 (d), 53.1 (t), 51.8 (d), 49.6 (t), 40.7 (d), 39.0 (t), 30.6 (t), 22.0 (t), 20.5 (q), 19.9 (q), 16.3 (q), 14.5 (t), 11.3 (q) ppm. ESI-MS: *m*/*z* (%): 476.38 $[M + 1]^+$ (100), 498.26 $[M + Na]^+$ (29), 514.33 $[M + K]^+$ (3). HPLC: t_R = 20.4 and 21.7 min (75% pure). Elemental analysis (%) calcd. for $C_{25}H_{37}N_3O_6$ (475.58): C 63.14, H 7.84, N 8.84; found: C 63.16, H 7.81, N 8.90.

(Butylcarbamoyl-*p*-tolylmethyl)-7-*endo*-BTG-Gly-NHEt (6): Compound **6** was prepared by use of Fmoc-Gly-OH as the first amino acid and *p*-tolylboronic acid for the Petasis reaction. The crude peptide was purified by flash column chromatography [EtOAc/petroleum ether (4:1), 0.1% Et_3N, R_f = 0.2] to give pure **6** (17 mg, 22%) as a mixture of two diastereomers in 49% *de*. ^{1}H NMR ($CDCl_3$, 200 MHz) major diastereomer: δ = 8.19 (m, 1 H), 7.14 (m, 4 H), 6.30 (m, 1 H), 6.20 (m, 1 H), 5.44 (s, 1 H), 4.64 (m, 1 H), 4.51 (d, $^3J_{H,H}$ = 6.1 Hz, 1 H), 4.02 (m, 2 H), 3.89 (s, 1 H), 3.40–3.21 (m, 2 H), 3.18–3.11 (m, 3 H), 2.79 (m, 1 H), 2.62 (d, $^2J_{H,H}$ = 11.0 Hz, 1 H), 2.33 (s, 3 H), 2.12 (d, $^2J_{H,H}$ = 11.3 Hz, 1 H), 1.54–1.34 (m, 2 H), 1.30–1.10 (m, 5 H), 0.95–0.83 (m, 3 H) ppm. ^{13}C NMR ($CDCl_3$, 50.33 MHz) major diastereomer: δ = 170.6 (s), 168.3 (s), 164.1 (s), 138.1 (s), 134.5 (s), 129.4 (d, 2 C), 128.8 (d, 2 C), 100.6 (d), 78.2 (d), 74.5 (d), 73.1 (d), 53.1 (t), 51.6 (t), 43.3 (t), 39.6 (t), 34.7 (t), 31.7 (t), 21.3 (q), 20.2 (t), 15.0 (q), 13.9 (q) ppm. MS: *m*/*z* (%): 446 $[M]^+$ (2.5), 347 (100), 273 (22). HPLC: t_R = 16.0 and 16.3 min (99% pure). Elemental analysis (%) calcd. for $C_{23}H_{34}N_4O_5$ (446.54): C 61.86, H 7.67, N 12.55; found: C 61.78, H 7.70, N 12.46.

(Butylcarbamoyl-*p*-tolylmethyl)-7-*endo*-BTG-Val-NHBn (7): Compound **7** was prepared by use of Fmoc-Val-OH as the first amino acid and *p*-tolylboronic acid for the Petasis reaction. The cleavage was performed with a solution of $BnNH_2$ (2.3 mL, 1.7 mmol) and H_2O (450 μL) in THF (1.5 mL), by stirring the mixture at room temperature for 12 h. The solution was drained and concentrated in vacuo to give a crude oil that was dissolved in dry CH_2Cl_2 (1 mL) and added dropwise to a solution of tartaric anhydride (367 mg, 1.7 mmol) in dry CH_2Cl_2 (1 mL). The mixture was stirred under N_2 at room temperature for 4 h, and was then quenched with H_2O and concentrated in vacuo. The solid obtained was dissolved in MeOH and eluted through Ambersep-OH resin. The solution was again concentrated in vacuo to give crude **8**, which was purified by flash column chromatography [EtOAc/petroleum ether (2:1), 0.1% Et_3N, R_f = 0.1], affording **7** (7 mg, 7%) as mixture of two diastereomers in 30% *de*. ^{1}H NMR ($CDCl_3$, 200 MHz) major diastereomer: δ = 8.28 (br s, 1 H), 7.67 (br s, 1 H), 7.40–7.04 (m, 9 H), 6.18 (br s, 1 H), 5.38 (s, 1 H), 4.83–4.31 (m, 3 H), 4.18–4.10 (m, 2 H), 3.56 (s, 1 H), 3.26–3.19 (m, 2 H), 3.16–2.85 (m, 2 H), 2.69–2.53 (m, 1 H), 2.33 (s, 3 H), 2.17 (m, 1 H), 1.59–1.46 (m, 2 H), 1.25–1.04 (m, 3 H), 0.92–0.81 (m, 9 H) ppm. ^{13}C NMR ($CDCl_3$, 50.33 MHz) major diastereomer: δ = 170.2 (s), 169.0 (s), 168.4 (s), 138.6 (s), 137.9 (s), 136.8 (s), 129.3 (d, 2 C), 128.8 (d, 2 C), 128.3 (d, 2 C), 128.1 (d, 2 C), 122.2 (d), 100.4 (d), 83.2, 62.4, 60.6, 58.1, 56.1, 53.8, 43.6, 39.5, 39.3, 29.9, 21.3, 20.3, 13.9 ppm. MS: *m*/*z* (%): 550 $[M]^+$ (0.05), 450 (11), 351 (100). HPLC: t_R = 20.5 and 21.0 min (88% pure). Elemental analysis (%) calcd. for $C_{31}H_{42}N_4O_5$ (550.69): C 67.61, H 7.69, N 10.17; found: C 67.68, H 7.65, N 10.11.

(Butylcarbamoyl-*p*-chlorophenylmethyl)-7-*endo*-BTG-Phe-NHEt (8): Compound **8** was prepared by use of Fmoc-Phe-OH as the first amino acid and *p*-Cl-phenylboronic acid for the Petasis reaction. The crude peptide was purified by flash column chromatography [EtOAc/petroleum ether (2:1), 0.1% Et_3N, R_f = 0.1] to give **8** (15 mg, 16%) as a mixture of two diastereomers in 20% *de*. ^1H NMR ($CDCl_3$, 200 MHz) major diastereomer: δ = 7.76 (d, $^2J_{H,H}$ = 7.2 Hz, 1 H), 7.34–7.13 (m, 9 H), 6.91 (brs, 1 H), 6.42 (brs, 1 H), 5.45 (s, 1 H), 4.64–4.48 (m, 3 H), 3.70 (m, 1 H), 3.28–2.96 (m, 6 H), 2.80 (m, 1 H), 2.61–2.31 (m, 2 H), 2.15–2.04 (m, 1 H), 1.64–1.49 (m, 4 H), 1.32–1.19 (m, 3 H), 0.99–0.86 (m, 3 H) ppm. ^{13}C NMR ($CDCl_3$, 50.33 MHz) major diastereomer: δ = 170.0 (s), 169.7 (s), 169.0 (s), 136.5 (s), 134.2 (s), 132.8 (s), 130.2 (d, 2 C), 129.2 (d, 2 C), 129.0 (d, 2 C), 128.8 (d, 2 C), 128.6 (d), 100.4 (d), 74.4 (d), 73.8 (d), 55.1 (t), 54.9 (d), 53.2 (d), 51.4 (t), 39.6 (t), 39.0 (t), 34.6 (t), 31.8 (t), 20.4 (t), 14.7 (q), 13.9 (q) ppm. MS: *m*/*z* (%): 559 $[M + 2]^+$ (0.3), 557 $[M]^+$ (1), 458 (45), 456 (100), 385 (3.8), 383 (9.3). HPLC: t_R = 20.5 and 21.0 min (88% pure). Elemental analysis (%) calcd. for $C_{29}H_{37}ClN_4O_5$ (557.08): C 62.52, H 6.69, N 10.06; found: C 62.61, H 6.71, N 10.12.

Computational Methods: Molecular-mechanics calculations were carried out on a SGI IRIX 6.5 workstation, with use of MacroModel (v6.5) molecular modelling software[26] with $MM2^+$ as a force field and the implicit chloroform GB/SA solvation system.[25] Full unconstrained Monte Carlo conformational searches[15] were carried out with use of a ring-closure for the six- and seven-membered rings of bicyclic structure. 2000 structures were generated and minimized until the gradient was less than 0.05 kJ·Å^{-1}·mol^{-1} with use of the TNCG gradient implemented in MacroModel.[27] All conformers with energies of 6 kcal mol^{-1} above the global minimum conformer were discarded. The Monte Carlo/Stochastic Dynamics (MC/SD) hybrid simulation algorithm[23] was used to assess the stabilities of low-energy conformers. A time step of 0.75 fs was used for the stochastic dynamics part of the algorithm. The MC simulation used random torsional rotations between ±60° and ±180° for all rotatable bonds except for the amide ones, where the random rotations were between ±90° and ±180°. No rotations were applied to the bonds of the scaffold. The total simulation was 2000 ps, and samples were taken at 1 ps intervals, yielding 2000 conformations for analysis. MC/SD algorithm gave percentage values weighted by the energetic contents of structures found, according to the Boltzmann law.

Acknowledgments

The authors thanks the Università degli Studi di Firenze and the MIUR for financial support. Ente Cassa di Risparmio di Firenze is gratefully acknowledged for contributing the 400-MHz NMR spectrometer. Ms. Brunella Innocenti and Mr. Maurizio Passaponti are acknowledged for technical support.

[1] a) G. Müller, *Angew. Chem. Int. Ed. Engl.* **1996**, *35*, 2767–2769; b) R. L. Stanfield, T. M. Fieser, R. A. Lerner, I. A. Wilson, *Science* **1990**, *248*, 712–719; c) C. M. Wilmot, J. M. Thorton, *J. Mol. Biol.* **1988**, *203*, 221–232; d) G. D. Rose, L. M. Gierasch, J. A. Smith, *Adv. Prot. Chem.* **1985**, *37*, 1–109.

[2] See, for example: a) H. B. Lee, M. Pattarawarapan, S. Roy, K. Burgess, *Chem. Commun.* **2003**, 1674–1675; b) A. Golebiowski, S. R. Klopfenstein, X. Shao, J. J. Chen, A.-O. Colson, A. L. Grieb, A. F. Russell, *Org. Lett.* **2000**, *2*, 2615–2617; c) M. A. Estiarte, M. Rubiralta, A. Diez, M. Thormann, E. Giralt, *J. Org. Chem.* **2000**, *65*, 6992–6999; d) A. J. Souers, A. A. Virgilio, Å. Rosenquist, W. Fenuik, J. A. Ellman, *J. Am. Chem. Soc.* **1999**, *121*, 1817–1825; e) N. Cho, M. Harada, T. Imaeda, T. Imada, H. Matsumoto, Y. Hayase, S. Sasaki, S. Furuya, N. Suzuki, S. Okubo, K. Ogi, S. Endo, H. Onda, M. Fujino, *J. Med. Chem.* **1998**, *41*, 4190–4195; f) B. E. Fink, P. R. Kym, J. A. Katzenellenbogen, *J. Am. Chem. Soc.* **1998**, *120*, 4334–4344; g) M. J. Genin, R. L. Johnson, *J. Am. Chem. Soc.* **1992**, *114*, 8778–8783.

[3] a) R. M. van Well, L. Marinelli, C. Altona, K. Erkelens, G. Siegal, M. van Raaij, A. L. Llamas-Saiz, H. Kessler, E. Novellino, A. Lavecchia, J. H. van Boom, M. Overhand, *J. Am. Chem. Soc.* **2003**, *125*, 10822–10829; b) E. Alonso, F. López-Ortiz, C. Del Pozo, E. Peralta, A. Macías, J. González, *J. Org. Chem.* **2001**, *66*, 6333–6338; c) D. Ranganathan, V. Haridas, S. Kurur, A. Thomas, K. P. Madhusudanan, R. Nagaraj, A. C. Kunwar, A. V. S. Sarma, I. L. Karle, *J. Am. Chem. Soc.* **1998**, *120*, 8448–8460; d) S. Hanessian, G. McNaughton-Smith, H.-G. Lombart, W. D. Lubell, *Tetrahedron* **1997**, *53*, 12789–12854.

[4] a) A. J. Souers, J. A. Ellman, *Tetrahedron* **2001**, *57*, 7431–7448; b) M. Eguchi, M. S. Lee, H. Nakanishi, M. Stasiak, S. Lovell, M. Kahn, *J. Am. Chem. Soc.* **1999**, *121*, 12204–12205; c) A. A. Virgilio, J. A. Ellman, *J. Am. Chem. Soc.* **1994**, *116*, 11580–11581.

[5] a) H. B. Lee, M. C. Zaccaro, M. Pattarawarapan, S. Roy, H. U. Saragovi, K. Burgess, *J. Org. Chem.* **2004**, *69*, 701–713; b) X. Gu, J. Ying, R. S. Agnes, E. Navratilova, P. Davis, G. Stahl, F. Porreca, H. I. Yamamura, V. J. Hruby, *Org. Lett.* **2004**, *6*, 3285–3288; c) L. Belvisi, A. Bernardi, A. Checchia, L. Manzoni, D. Potenza, C. Scolastico, M. Castorina, A. Cupelli, G. Giannini, P. Carminati, C. Pisano, *Org. Lett.* **2001**, *3*, 1001–1004; d) A. J. Souers, A. A. Virgilio, S. S. Schürer, J. A. Ellman, T. P. Kogan, H. E. West, W. Ankener, P. Vanderslice, *Bioorg. Med. Chem. Lett.* **1998**, *8*, 2297–2302; e) B. Gardner, H. Nakanishi, M. Kahn, *Tetrahedron* **1993**, *49*, 3433–3448.

[6] a) A. Guarna, A. Guidi, F. Machetti, G. Menchi, E. G. Occhiato, D. Scarpi, S. Sisi, A. Trabocchi, *J. Org. Chem.* **1999**, *64*, 7347–7364; b) D. Scarpi, E. G. Occhiato, A. Trabocchi, R. J. Leatherbarrow, A. B. E. Brauer, M. Nievo, A. Guarna, *Bioorg. Med. Chem.* **2001**, *9*, 1625–1632; c) A. Trabocchi, E. G. Occhiato, D. Potenza, A. Guarna, *J. Org. Chem.* **2002**, *67*, 7483–7492; d) A. Trabocchi, G. Menchi, F. Guarna, F. Machetti, D. Scarpi, A. Guarna, *Synlett* **2006**, *3*, 331–353.

[7] A. Trabocchi, D. Potenza, A. Guarna, *Eur. J. Org. Chem.* **2004**, 4621–4627.

[8] D. Scarpi, D. Stranges, A. Trabocchi, A. Guarna, *Tetrahedron* **2006**, *62*, 1575–1582.

[9] a) N. A. Petasis, I. A. Zavialov, *J. Am. Chem. Soc.* **1997**, *119*, 445–446; b) N. A. Petasis, A. Goodman, I. A. Zavialov, *Tetrahedron* **1997**, *53*, 16463–16470.

[10] a) S. R. Klopfenstein, J. J. Chen, A. Golebiowski, M. Li, S. X. Peng, X. Shao, *Tetrahedron Lett.* **2000**, *41*, 4835–4839; b) N. Schlienger, M. R. Bryce, T. K. Hansen, *Tetrahedron* **2000**, *56*, 10023–10030.

[11] A. Golebiowski, S. R. Klopfenstein, J. J. Chen, X. Shao, *Tetrahedron Lett.* **2000**, *41*, 4841–4844.

[12] a) J. Yang, S. H. Gellman, *J. Am. Chem. Soc.* **1998**, *120*, 9090–9091; b) G.-B. Liang, C. J. Rito, S. H. Gellman, *J. Am. Chem. Soc.* **1992**, *114*, 4440–4442; c) S. H. Gellman, G. P. Dado, G.-B. Liang, B. R. Adams, *J. Am. Chem. Soc.* **1991**, *113*, 1164–1173; d) G. Boussard, M. Marraud, *J. Am. Chem. Soc.* **1985**, *107*, 1825–1828.

[13] V. Sieber, G. R. Moe, *Biochemistry* **1996**, *35*, 181–188.

[14] T. S. Haque, J. C. Little, S. H. Gellman, *J. Am. Chem. Soc.* **1996**, *118*, 6975–6985.

[15] G. Chang, W. C. Guida, W. C. Still, *J. Am. Chem. Soc.* **1989**, *111*, 4379–4386.

[16] A. Trabocchi, G. Menchi, M. Rolla, F. Machetti, I. Bucelli, A. Guarna, *Tetrahedron* **2003**, *59*, 5251–5258.

[17] V. Krchnák, J. Vágner, P. Sáfar, M. Lebl, *Collect. Czech. Chem. Commun.* **1998**, *53*, 2542–2548.

[18] M. E. Attardi, G. Porcu, M. Taddei, *Tetrahedron Lett.* **2000**, *41*, 7391–7394.

[19] Early cleavage after treatment of the resin-bound active ester group with amine was checked by analysis of filtrate, resulting in complete stability of the resin-bound compound to this reaction step. It was supposed that the resistance of resin-bound product to early cleavage by amine treatment was mainly due to the amount of amine used in the two steps, as in the amidation reaction only 5 equiv. were used, whereas in the cleavage the amount of amine was raised to 110 equiv.
[20] a) K. K. Nanda, B. W. Trotter, *Tetrahedron Lett.* **2005**, *46*, 2025–2028; b) T. Koolmeister, M. Södergren, M. Scobie, *Tetrahedron Lett.* **2002**, *43*, 5969–5970.
[21] Diastereoselectivity was determined immediately after the Petasis reaction by treatment of the resulting COOH group with TMS/diazomethane in CH_2Cl_2/MeOH as solvent system for 2 h, followed by cleavage from the resin. The resulting *de* value of 87% was consistent with a lack of epimerization during the COOH activation with DIC/HOBt.
[22] The conformational analysis on major diastereomers of **2** and **4** were performed on enriched mixtures of such compounds.
[23] F. Guarnieri, W. C. Still, *J. Comput. Chem.* **1994**, *15*, 1302–1310.
[24] L. Belvisi, C. Gennari, A. Madder, A. Mielgo, D. Potenza, C. Scolastico, *Eur. J. Org. Chem.* **2000**, 695–699.
[25] W. C. Still, R. C. Tempczyk, R. C. Hawley, T. Hendrickson, *J. Am. Chem. Soc.* **1990**, *112*, 6127–6129.
[26] F. Mohamadi, N. G. J. Richards, W. C. Guida, R. Liskamp, M. Lipton, C. Caufield, G. Chang, T. Hendrickson, W. C. Still, *J. Comput. Chem.* **1990**, *11*, 440–467.
[27] J. W. Ponder, F. M. Richards, *J. Comput. Chem.* **1987**, *8*, 1016–1024.

Received: July 26, 2006
Published Online: February 9, 2007

